INTERNATIONAL JOURNAL FOR NUMERICAL METHODS IN FLUIDS, VOL. 6, 1–19 (1986)

A STUDY OF PENALTY ELEMENTS FOR INCOMPRESSIBLE LAMINAR FLOWS

GOURI DHATT* AND GUY HUBERT†

UTC, Department de Genie Mecanique BP 233, 60 206 Compiegne, France

SUMMARY

A finite element model is developed based on the penalty formulation to study incompressible laminar flows. The study includes a number of new quadrilateral and triangular elements for 2-dimensional flows and a number of new hexahedral and tetrahedral elements for 3-dimensional flows. All elements employ continuous velocity approximations and discontinuous pressure approximations respecting the LBB condition of numerical instability. An incremental Newton–Raphson method coupled with the Broyden method is used to solve the non-linear equations. Several numerical examples (colliding flow, cavity flow, etc.) are presented to assess the efficiency of elements.

INTRODUCTION

A large number of research groups from universities and industry alike are actively involved with the development of finite element codes for solving incompressible viscous flow problems. In order to solve effectively real life turbulent flow, it is essential to develop efficient numerical solvers for laminar problems, which is in effect the purpose of the present study. The main difficulties in solving such flows via finite elements lie in proper choice of a variational model, proper choice of finite element approximations taking into account the incompressibility constraint, and the choice of a solution strategy for solving highly non-linear large systems of equations.

The mathematical formulation of the problem is based on the Navier–Stokes equations employing the primitive variables, velocity and pressure, along with the incompressibility constraint. The finite element model is obtained through the weighted residual method employing Galerkin type weighting functions.[1] One type of finite element discretization employs the C^0 pressure approximation (continuous) which has been the object of earlier finite element applications.[2–5] The other type employs discontinuous local pressure approximation using a variational penalty model.[6–9] In our study, we are particularly interested in the penalty formulation employing a discontinuous pressure approximation, since it leads to a better conditioning of the discretized system and a reduced number of degrees of freedom containing only velocity variables as unknowns, the pressure variables being eliminated at the element level through static condensation.

The finite element discretization of incompressible models requires that the approximations for velocity and pressure (continuous or local) should satisfy certain consistency conditions in order to obtain convergent stable solutions. The recent works of Ladyszenskaya,[10] Brezzi[11]

*Professor, Civil Engineering, Laval University, Québec, Canada and Mechanical Engineering, University of Compiègne, Compiègne, France.

†Research Engineer, Compiègne Science-Industrie, University of Compiègne, France

0271–2091/86/010001–19$01.90

Received 6 November 1984
Revised 28 June 1985

and Babuska[12] (LBB) permit us to define the consistency conditions in a precise mathematical form adapted to finite element approximations. Though the mathematical form of these conditions, often known as the LBB condition, is quite straightforward, its explicit verification for different types of elements could be a difficult and cumbersome exercise.

Taylor and Hood[5] may be considered among the first group of researchers to employ the velocity–pressure (C^0-approximation) formulation for solving two-dimensional laminar flows with quadrilateral elements. Through brutal numerical experimentation, they have identified the consistency condition for their model leading to a choice of bilinear pressure field (4 nodes) and biquadratic velocity field (9 nodes) for obtaining stable solutions. We may mention works of Taylor and Hood,[5] Malkus and Hughes[3] and Cochet,[2] among others, which deal with the choice of velocity–pressure approximations (C^0) for two-dimensional flows.

The penalty formulation was first presented by Zienkiewicz[13] for a quadrilateral element under a rather restricted form of reduced integration technique. In later works,[6,7] the penalty formulation was presented in a general form under the name of the consistent penalty model, where the pressure approximation is unrelated to the number of numerical integration points employed and the verification of the LBB condition is presented in an explicit manner. The penalty formulation with discontinuous pressure field has been the object of various recent works, especially by Sani *et al.*,[7] Oden,[8] Dhatt and Hubert[6] and, in free surface flows, by Zienkiewicz and Heinrich[9] and Cochet *et al.*[14]

Oden *et al.*[15] and Reddy[16] employ functional analysis techniques to present the penalty formulation in a general context along with the LBB condition. The verification of this condition for a given finite element approximation is a difficult and cumbersome task. In a recent article, Fortin[17] proposed a simple technique of verification for elements with discontinuous pressure approximation.

The trick is to show an equivalence of the discrete version of the LBB condition for a given element with the continuous version, knowing that it is well respected by the continuous model. In the present study, we shall employ this technique to verify the LBB condition for various types of two- and three-dimensional elements.

The solution strategies for solving highly non-linear equations may be classified into two groups. The engineering group primarily employs a version of a Newton-type method for solving non-linear equations. A general solution strategy based on Newton-type methods may employ simultaneously a Newton–Raphson incremental technique,[2] a quasi-Newton technique, especially the Broyden method,[18–20] and certain forms of line search technique. The numerical analysis group, mainly pioneered by Glowinski and Periaux[21,22] employs a conjugate-gradient technique with iterative decoupling of velocity components. The solution direction is predicted through a scalar Laplacian operator, employing the technique of conjugate gradients with a least-squares preconditioning. At present, the major problem is that of solving large three-dimensional problems; no clear direction has so far emerged. The present authors feel that an efficient three-dimensional solution technique will include simultaneously some sort of decomposition in space as well as in variables and a version of the Newton method along with conjugate gradients. However in this study, we shall be using a version of a Newton-type method for solving the non-linear equations.

VARIATIONAL FORMULATION

The Navier–Stokes equations are

$$u_j u_{i,j} + \frac{1}{\rho} p_{,i} - \tau_{ij,j} = f_i, \quad \text{on} \quad V, i = 1,2,3, \tag{1a}$$

$$\operatorname{div} \mathbf{u} = (u_{j,j}) = 0 \tag{1b}$$

(with summation on $j = 1,2,3$),

$$u_i = u_{is} \text{ on } S_u \text{ or } \tau_{ij} l_j - \frac{p l_i}{\rho} = f_{is} \text{ on } S_f$$

and

$$u_{i,j} = \partial u_i / \partial x_j; \quad \tau_{ij} = \nu(u_{i,j} + u_{j,i})$$

where

$\mathbf{u}$ is the velocity vector with component u_1, u_2, u_3
τ_{ij} are the components of the stress tensor
p is the pressure
ν is the kinetic viscosity, may include the turbulent viscosity
ρ is the mass density
f_i is the volume force
V is the geometrical domain limited by the boundary S, $\mathbf{n}$ being the normal at the boundary oriented towards the exterior
l_i are the direction cosines of the normal n
x_1, x_2, x_3 are the Cartesian co-ordinates.

The variational model is obtained by using a weighted residual method[1,16] employing Galerkin-type weighting functions and performing integration by parts to reduce the maximum order of derivatives in the resultant expression (often called the 'weak' variational form):

$$W = \int_V \sum_{i=1}^{3} [v_i(u_j u_{i,j}) + v_{i,j}\tau_{ij} - v_i f_i - \frac{1}{\rho} p \operatorname{div} \mathbf{v}] \, dV - \int_{S_f} v_i f_{is} \, dS + \int_V q \operatorname{div} \mathbf{u} \, dV = 0 \qquad (2)$$

(terms are summed over j) and $u_i = u_{is}$, $v_i = 0$ on S_u where $u_i, v_i \in H^1(V)$ and $p, q \in L^2(V)$; H^1 represents the space of square-integrable functions such that $\int |u_i|^2 dV$, $\int (|\partial u_i / \partial x_j|^2) dV$ etc. $< \infty$, and L^2 represents functions such that $\int |p|^2 dV < \infty$. Note that all continuous approximations (C^0) belong automatically to H^1; all defined discontinuous functions belong to L^2. u_i, p represent velocity and pressure fields, v_i, q represent corresponding weighting functions.

For the penalty formulation, we define the incompressibility constraint (1b) in the following manner:

$$\operatorname{div} \mathbf{u} + \frac{p}{\lambda} = 0, \qquad (3)$$

where λ is a relatively large positive scalar such that p/λ is numerically zero for all practical purposes.

The *ad hoc* choice of equation (3) may be explained through physical as well as mathematical reasoning, both, in effect, expressing the same idea. We may assume that the fluid has large bulk modulus λ developing a significant pressure field with a relatively small compressibility defined by div $\mathbf{u}$.

From the mathematical point of view, one can add the penalty constraint $-(1/2)\int_V \lambda \delta (\operatorname{div} \mathbf{u})^2 dV$ to equation (2), leading to $\lambda \operatorname{div} \mathbf{u} = -p$ in the sense of Lagrange multipliers, which is equivalent to modifying equation (2) by addition of $\int_V (qp/\lambda) dV$ (for further details, consult Reference 16).

Using (2), the penalty variational form is written as

$$W_p = W + \int_V qp/\lambda \, dV = 0$$

and (4)

$$u_i = u_{is}, v_i = 0 \quad \text{on} \quad S_u.$$

Notice that the contour S_f in (2) allows us to introduce the force or pressure boundary values. For example, on inlet, we may have $\partial u_i/\partial n = 0$, $p = \bar{p}$, then $f_{is} = -\bar{p}l_i/\rho$ gives an equivalent load vector.

We should also ensure that the model (2) or (4) is equivalent to (1) in the variational sense. Without going into details, the equivalence for Stokes' problem (neglecting non-linear convection terms) is assured if the continuous version of the LBB condition is satisfied:

$$\sup_{v\in H_0^1} \frac{\int_V q \operatorname{div} \mathbf{v}\, dV}{\|v\|_{H_0^1}} \geqslant a\|q\|_{L^2}, \quad a>0, \quad \forall q\in L^2, \tag{5}$$

where H_0^1 is the space of H^1 functions which are zero on the boundary and $\|\cdot\|$ is the corresponding norm.

FINITE ELEMENT DISCRETIZATION

Owing to the incompressibility constraint, the velocity–pressure approximation must satisfy the discrete LBB condition for a convergent stable solution, i.e.

$$\sup_{v_h\in V_h} \frac{\int_V q_h \operatorname{div} \mathbf{v}_h\, dV}{\|v_h\|_{V_h}} \geqslant b\|q_h\|, \quad \forall q_h\in Q_h, \tag{6}$$

where q_h, v_h are finite element approximations defining the spaces Q_h, V_h belonging to L^2, H^1, respectively.

Experience has shown that the verification of the LBB condition in the form of equation (6) involves cumbersome, perhaps unnecessary, algebraic manipulations. Based on recent work of Fortin, we may present this condition in another form. Profiting from the fact that the variational model of a problem satisfies equation (5), the discrete LBB condition may be written in the following alternative form:

$$\int_V q_h \operatorname{div} \mathbf{v}_h\, dV = \int_V q_h \operatorname{div} \mathbf{v}\, dV, \quad \forall q_h\in Q_h, \quad v_h\in V_h. \tag{7}$$

We shall present in the following section, a number of elements, two- and three-dimensional, for solving Navier–Stokes equations which satisfy equation (7).

PRESENTATION OF ELEMENTS

Using a finite element approximation, the expression (4) becomes

$$W_p = \sum_{\text{element}} W_p^e = 0. \tag{8}$$

In discretized form:

$$W_p^e = \langle v_n, q_n\rangle \left([\bar{\mathbf{k}}] \begin{Bmatrix} u_n \\ p_n \end{Bmatrix} - \begin{Bmatrix} f_u \\ 0 \end{Bmatrix} \right), \tag{9}$$

where $\bar{\mathbf{k}}$ is an element non-linear matrix; u_n, p_n are element nodal or non-nodal degrees of freedom; f_u is the element excitation and v_n, q_n are corresponding arbitrary weighting coefficients.

In an assembled form:

$$W_p = \langle \mathbf{V}_n \rangle ([\mathbf{K}]\{\mathbf{U}_n\} - \{\mathbf{F}_n\}) = 0$$

or

$$\{R(\mathbf{U}_n)\} = [\mathbf{K}]\{\mathbf{U}_n\} - \{\mathbf{F}_n\} = 0, \quad \text{for all} \quad \mathbf{V}_n, \tag{10}$$

where $[\mathbf{K}]$ is an assembled non-linear global matrix taking into account various boundary conditions, $\{\mathbf{F}\}$ is the corresponding load vector and $\mathbf{U}_n$ are the global velocity unknowns, the pressure coefficients being eliminated at the element level.

The finite element approximation is written in the following symbolic form:

$$u_1 = \langle \mathbf{N} \rangle \{\mathbf{u}_{1n}\}, \quad v_1 = \langle \mathbf{N} \rangle \{\mathbf{v}_{1n}\}, \tag{11a}$$

$$p = \langle \mathbf{N}_p \rangle \{\mathbf{p}_n\}, \quad q = \langle \mathbf{N}_p \rangle \{\mathbf{q}_n\}. \tag{11b}$$

Approximations for $u_2, v_2; u_3, v_3$ are similar to (11a). The element matrix is written as:

$$[\bar{\mathbf{k}}] = \begin{bmatrix} \mathbf{b} & -\mathbf{c} \\ +\mathbf{c}^T & +\mathbf{m}/\lambda \end{bmatrix}, \tag{12a}$$

where $[\mathbf{b}]$ is a non-linear matrix coupling only velocity terms,

$$[\mathbf{c}] = \int_V \begin{Bmatrix} \mathbf{N}_{,x_1} \\ \mathbf{N}_{,x_2} \\ \mathbf{N}_{,x_3} \end{Bmatrix} \langle \mathbf{N}_p \rangle \, dV, \tag{12b}$$

$$[\mathbf{m}] = \int_V \{\mathbf{N}_p\} \langle \mathbf{N}_p \rangle \, dV. \tag{12c}$$

For discontinuous pressure approximations, the penalty formulation allows us to eliminate the pressure terms by static condensation and obtain an element matrix in terms of velocity variables only:

$$[\mathbf{k}] = [\mathbf{b}] + \lambda [\mathbf{c}][\mathbf{m}^{-1}][\mathbf{c}^T]. \tag{13}$$

In order to present the LBB condition in terms of a matrix rank, we write the assembled

Table I. Triangular elements (5 different elements)

Symbols	Nodes	Velocity approximation	Local pressure approximation	Element d.o.f.	Element d.o.f. after condensation
T6C	6	Quadratic for u_1, u_2	Constant	13	12
T6NC	6	Incomplete quadratic for u_1, u_2; u_1, u_2 at each corner node normal component at mid-side nodes	Constant	10	9
T7L	plus one internal node	Quadratic plus a cubic bubble function	$p = a_1 + a_2\xi + a_3\eta$	17	12
T7NL	16 plus one internal node	Incomplete quadratic as T6NC, plus a cubic bubble function	Linear	14	9

Table II. Quadrilateral elements (6 different elements)

Symbols	Nodes	Velocity approximation	Local pressure approximation	Element d.o.f.	Element d.o.f. after condensation
Q8C	8	Lagrange incomplete	Constant	17	16
Q8NC	8	Approximation uses 2 velocity components at each corner node and one normal velocity component at each mid-side node	Constant	13	12
Q9L	8 plus one internal node	Biquadratic	Bilinear, does not respect LBB condition, if 4 Gauss points are used for integration, identical to reduced integration element	22	16
Q9L	8 plus one internal node	Biquadratic	$p = a_1 + a_2\xi + a_3\eta$	21	16
Q9NL	9	Approximation as Q8NC plus one bubble function	$p = a_1 + a_2\xi + a_3\eta$	17	12

Table III. Hexahedral elements (2 elements)

Symbols	Nodes	Velocity approximation	Local pressure approximation	Element d.o.f.	Element d.o.f. after condensation
H8N	8 corner nodes plus one at centre of each face	u_1, u_2, u_3 at each corner node, normal component at other six mid-face nodes	Constant	31	30
H27L	26 plus one internal node	Triquadratic	Linear $a_1 + a_2\xi + a_3\eta + a_4\zeta$	85	78

version of (12) keeping pressure coefficients:

$$\begin{bmatrix} \mathbf{B} & -\mathbf{C} \\ +\mathbf{C}^{\mathrm{T}} & +\mathbf{M}/\lambda \end{bmatrix} \begin{Bmatrix} \mathbf{U}_n \\ \mathbf{P}_n \end{Bmatrix} = \{\mathbf{F}_0\}. \tag{14}$$

In order that equation (14) leads to a numerically stable solution for $\mathbf{U}_n, \mathbf{P}_n$, the following condition should be satisfied (a version of the LBB condition):

If r is the total number of coefficients $\mathbf{P}_n$, then the rank of the matrix [**C**] must be equal to $(r-1)$. In other words, the matrix [**C**] must have $(r-1)$ independent eigenvectors or $(r-1)$ non-zero eigenvalues. It is implicitly assumed that the rank of the matrix [**B**] is equal to number of unknowns $\{\mathbf{U}_n\}$.

Table IV. Proposed tetrahedral elements (2 elements)

Symbols	Nodes	Velocity approximation	Local pressure approximation	Element d.o.f.	Element d.o.f. after condensation
T8N	4 corner nodes plus one at centre of each face	u_1, u_2, u_3 at each corner node, normal component at four mid-face nodes	Constant	17	16
T13L	14 plus one internal node	Quadratic	Linear	49	42

We may remark that to verify explicitly the rank of [C] using only the elementary matrices [c] for a general element geometry is a highly difficult task, if not impossible. However, in certain cases, the use of equations (6) or (7) may lead to a simple explicit verification of the LBB condition.

The main characteristics of the different two- and three-dimensional elements proposed are described in Tables I–IV. All these elements respect the LBB condition unless indicated otherwise.

Bidimensional elements with constant pressure

The velocity approximations for T6C and Q8C (see Tables I and II) are standard quadratic and incomplete biquadratic functions.[1] The discontinuous pressure representation is constant over each element. The velocity approximations for T6NC and Q8NC, which have two velocity components at each corner node and a normal component at each mid-side node (Figures 1 and 2) are given as follows.

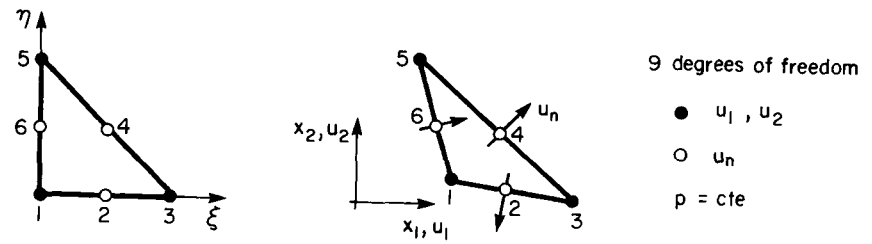

Figure 1. T6NC Element

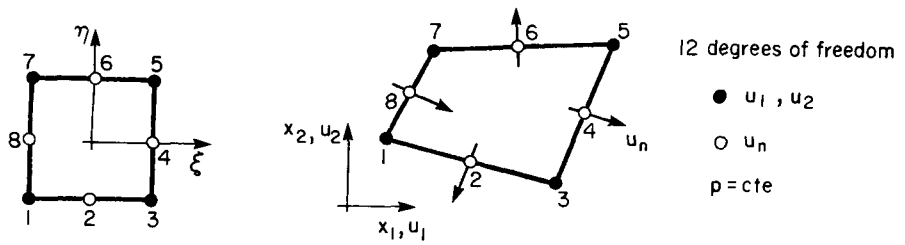

Figure 2. Q8NC Element

Table V.

Triangle			Quadrilateral		
j	k	m	j	k	m
1	2	6	1	2	8
3	4	2	3	4	2
5	6	4	5	6	4
			7	8	6

Elements T6NC and Q8NC

$$u_1(\xi,\eta) = \langle \mathbf{H}^1 \rangle \{\mathbf{u}_n\}; \quad \langle \mathbf{u}_n \rangle = \langle \underset{\text{corner node}}{u_1^{(1)} u_2^{(1)}} | \underset{\text{midside node}}{u_n^{(2)}} | \cdots \rangle, \tag{15}$$

$$u_2(\xi,\eta) = \langle \mathbf{H}^2 \rangle \{\mathbf{u}_n\},$$

$$\langle \mathbf{H}^i \rangle = \langle \cdots : \underset{\text{corner node}}{H^i_{j1}}, \underset{\text{midside node}}{H^i_{j2}}; H^i_{j+1} : \cdots \rangle, \quad \text{For each } i = 1,2$$

$j = 1,3,5$ for a triangular element and

$j = 1,3,5,7$ for a quadrilateral element.

The $\langle \mathbf{H}^i \rangle$ functions are:

For a corner node

$$\begin{aligned} H^1_{j1} &= N_j + \tfrac{1}{2}(s_k^2 N_k + s_m^2 N_m), \quad & H^2_{j1} &= -\tfrac{1}{2}(c_k s_k N_k + c_m s_m N_m), \\ H^1_{j2} &= -\tfrac{1}{2}(c_k s_k N_k + c_m s_m N_m), \quad & H^2_{j2} &= N_j + \tfrac{1}{2}(c_k^2 N_k + c_m^2 N_m). \end{aligned} \tag{16}$$

For a mid-side node

$$H^1_{j+1} = c_{j+1} N_{j+1}, \quad H^2_{j+1} = s_{j+1} N_{j+1}. \tag{17}$$

The values of j,k,m for triangular and quadrilateral shapes are defined as on Table V.

N_i are classical functions for the 6-node triangular element or the 8-node quadrilateral element.[1] The normal vector (c_k, s_k) is defined for each side of an element which is assumed straight. The unique $\mathbf{u}_n$ direction of each mid-side node sharing two elements is obtained by orientating the corresponding side from its corner node with the lower number to the one with higher number and fixing the normal at $-90°$. For these two elements, the matrix [**m**] (12c) is reduced to one term, and the matrix [**c**] to one vector.

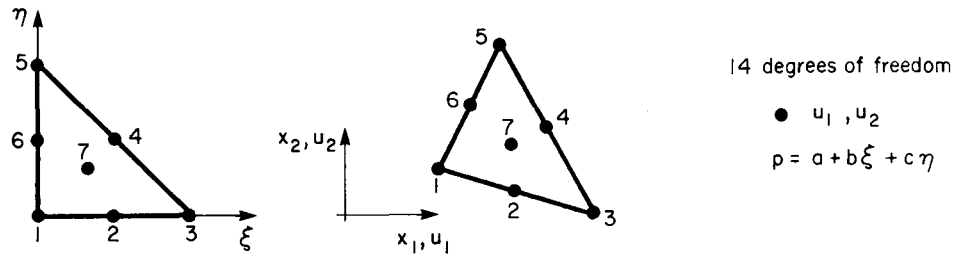

Figure 3. T7L Element

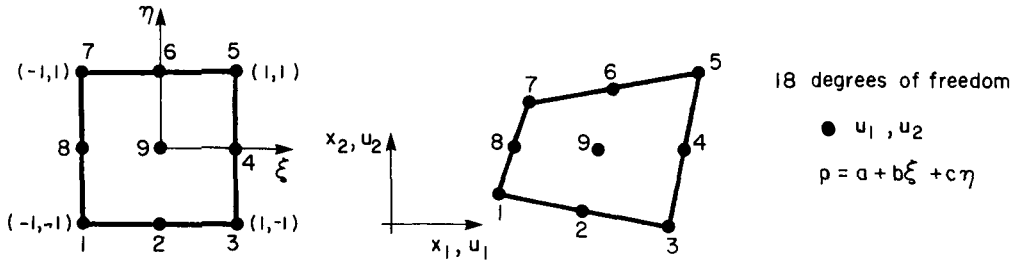

Figure 4. Q9L Element

Bidimensional elements with linear pressure

Element T7L. The velocity approximation is defined by (Figure 3):

$$
\begin{aligned}
u_1 &= \langle \mathbf{N}_{u_1} \rangle \{\mathbf{u}_n\}, \quad u_2 = \langle \mathbf{N}_{u_2} \rangle \{\mathbf{u}_n\}, \\
\langle \mathbf{u}_n \rangle &= \{\mathbf{u}_n\}^{\mathrm{T}} = \langle u_1^1, u_2^1, u_1^2, u_2^2, \ldots, u_1^7, u_2^7 \rangle, \\
\langle \mathbf{N}_{u_1} \rangle &= \langle N_1, 0, N_2, 0, \ldots, N_7, 0 \rangle, \\
\langle \mathbf{N}_{u_2} \rangle &= \langle 0, N_1, 0, N_2, \ldots, 0, N_7 \rangle, \\
N_i &= N_i^* + N_7/9 \text{ (corner node)}, \quad i = 1,3,5, \\
N_i &= N_i^* - 4N_7/9 \text{ (mid-side node)}, \quad i = 2,4,6, \\
N_7 &= 27\xi\eta(1 - \xi - \eta), \\
p &= a + b\xi + c\eta \text{ (generalized local approximation)},
\end{aligned}
\tag{18}
$$

N_i^* being the interpolation functions for a 6-node triangular element.[1]

Element Q9L. The velocity is identical to the 9-node quadrilateral element[1] (Figure 4) and the pressure is defined by a local linear approximation.

The approximations for the T7NL and Q9NL (Figures 5 and 6) elements are obtained in a manner similar to that employed for the elements T6NC and Q8NC with the addition of an internal node.

For T7L or T7LN elements, if the generalized pressure approximation is replaced by an

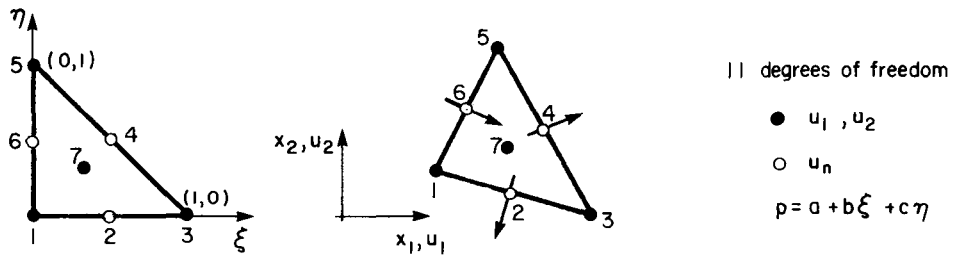

Figure 5. T7NL Element

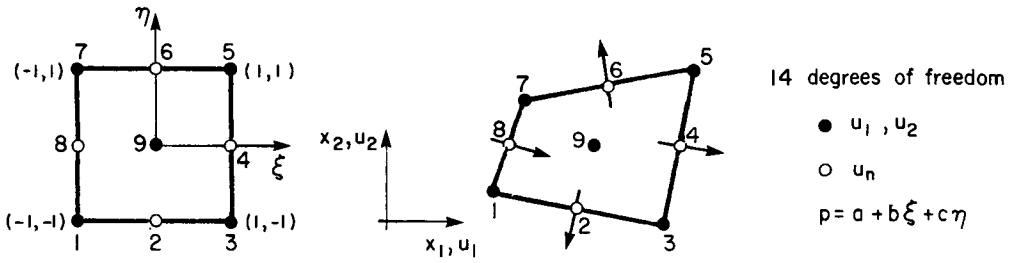

Figure 6. Q9NL Element

equivalent nodal approximation (Hammer integration points):

$$p = N_1 p_1 + N_2 p_2 + N_3 p_3$$
$$N_1 = 2(\lambda - \tfrac{1}{6}), \quad N_2 = 2(\xi - \tfrac{1}{6}), \quad N_3 = 2(\eta - \tfrac{1}{6}), \tag{19}$$

where $\lambda = 1 - \xi - \eta$.

The matrix [**m**] of equation (12c) becomes diagonal:

$$[\mathbf{m}] = A/3 \begin{bmatrix} 1 & 0 & 0 \\ 0 & 1 & 0 \\ 0 & 0 & 1 \end{bmatrix},$$

with A being the area of the element.

If the mesh is composed of rectangular elements for Q9L or Q9LN, the [**m**] matrix is given by

$$[\mathbf{m}] = A \begin{bmatrix} 1 & 0 & 0 \\ 0 & 1/3 & 0 \\ 0 & 0 & 1/3 \end{bmatrix},$$

where A is the area of the rectangle.

Tridimensional elements

In order to solve industrial three-dimensional problems, it is essential to develop efficient and simple three-dimensional elements. This field is at present attracting much attention and we shall see in the future research studies related to choice of elements, choice of solution methods and the use of parallel processors for solving real-life three-dimensional problems.

Element H8N. This element (Figure 7), satisfying the LBB condition (see Appendix), was

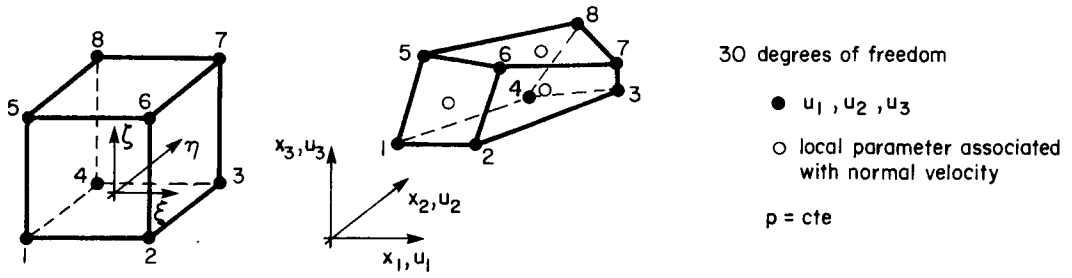

Figure 7. H8N Elememt

recently proposed by Fortin.[17] The pressure is constant over each element and the velocity approximation is

$$\begin{aligned} u_1 &= \langle \mathbf{N}_{u_1} \rangle \{u\} = \langle N_1,\ldots,N_8, 0,\ldots,0, 0,\ldots,0, \bar{N}_1 l_1, \bar{N}_2 l_2,\ldots,\bar{N}_6 l_6 \rangle, \\ u_2 &= \langle \mathbf{N}_{u_2} \rangle \{\mathbf{u}\} = \langle 0,\ldots,0, N_1,\ldots,N_8, 0,\ldots,0, \bar{N}_1 m_1, \bar{N}_2 m_2,\ldots,\bar{N}_6 m_6 \rangle, \\ u_3 &= \langle \mathbf{N}_{u_3} \rangle \{\mathbf{u}\} = \langle 0,\ldots,0, 0,\ldots,0, N_1,\ldots,N_8, \bar{N}_1 n_1, \bar{N}_2 n_2,\ldots,\bar{N}_6 n_6 \rangle, \end{aligned} \tag{20}$$

where

$\langle \mathbf{u} \rangle = \{\mathbf{u}\}^{\mathrm{T}} = \langle u_1^1,\ldots,u_1^8, u_2^1,\ldots,u_2^8, u_3^1,\ldots,u_3^8, \alpha_1,\ldots,\alpha_6 \rangle$.

l_i, m_i, n_i are direction cosines of the normal vector of the face i.

$N_1, N_2,\ldots,N_8$ are the classical functions of the trilinear hexahedral element.[1]

$\bar{N}_1,\ldots,\bar{N}_6$ are interpolation functions associated with the local parameters α_i of each face along the normal vector. The uniqueness of the normal direction for each face shared by two elements is essential. One can easily fix this direction by defining two vectors in each face, orientated from the lowest node number to higher node numbers. The choice of $\bar{N}_i$ is straightforward, for example, $\bar{N}_1$ of the face 1-2-3-4 is $(1-\xi^2)(1-\eta^2)(1-\zeta)$.

The normal components α_i associated with the faces of each element cannot be removed at element level, owing to the sharing of each face by two elements. It is believed that this may lead to an undesirable size of bandwidth, and thus to an effective reduction in the numerical efficiency of the element.

METHOD OF SOLUTION

The finite element approximation leads to a discretized model of flow problems written in the following matrix form:

$$[\mathbf{K}(\mathbf{u})]\{\mathbf{u}\} - \{\mathbf{F}\} = 0. \tag{21}$$

Equation (21) represents a non-linear system of equations, defining either stationary flow or non-stationary flow, the time derivative being discretized by a variant of the implicit integration formulae.[1]

In this study, we employ the incremental Newton method coupled with the quasi-Newton method of Broyden.[18–20] The solution strategy is based on the application of the Newton method till the norm $|\Delta u_i|/|u_i|$ is sufficiently small, followed by the application of the Broyden method to obtain desired convergence accuracy. This solution strategy is incorporated in the general finite element code MEF.[1]

NUMERICAL EXAMPLES

We present a number of numerical examples in order to demonstrate the reliability of various elements for two- and three-dimensional flows. For 2-D problems, we are interested to assess the efficiency of a family of new penalty triangular elements discussed in the previous sections. The presentation of 3-D elements may be considered as exploratory, believing that this will orientate our research efforts for the choice of elements, and the choice of solution strategies. All mesh generation and graphical processing employ the interactive code MOSAIC, developed at the University of Compiègne, compatible with the MEF.

Two-dimensional problems

Colliding flow. We study a simple Stokes flow over a unit square domain, using T7L, T7L* (same as T7L, with the elimination of two internal velocity components at the element level), T6NC and T6-3 (quadratic velocity with linear continuous pressure[2]).

The Stokes flow is defined by

$$\begin{aligned} -\Delta u_i + p_{,i} &= f_i \quad i = 1,2, \\ u_{i,i} &= 0, \\ u &= u_s \quad \text{on all four sides,} \end{aligned} \tag{22}$$

with $0 \leqslant x_1 \leqslant 1$; $0 \leqslant x_2 \leqslant 1$.

The exact solution of the flow is chosen as:

$$\begin{aligned} u_1 &= \sin x_2, u_2 = \sin x_1, \qquad p = \sin(x_1 + x_2), \\ f_1 &= \sin x_2 + \cos(x_1 + x_2), \quad f_2 = \sin x_1 + \cos(x_1 + x_2). \end{aligned} \tag{23}$$

We impose boundary velocity values obtained by the above equation.

For comparison purposes, we define the following error norms:

$$E_u = \sum_{i=1}^{n} \frac{|\sqrt{(u_1^2 + u_2^2)} - \sqrt{(u_{e1}^2 + u_{e2}^2)}|}{n},$$

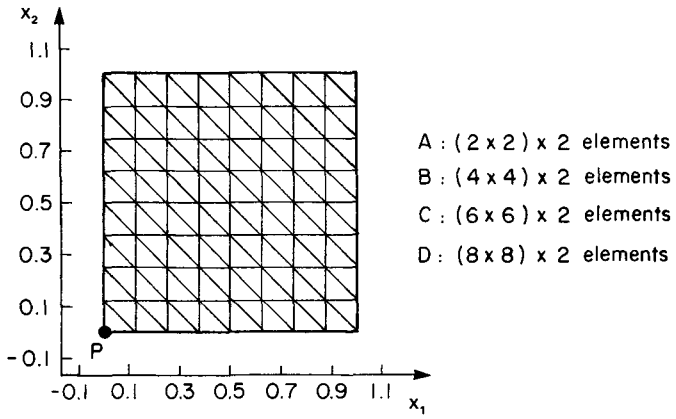

Elements	Mesh							
	A		B		C		D	
	B	N	B	N	B	N	B	N
T6 NC	3	34	11	106	18	218	27	370
T7L	8.5	66	28	226	41	482	55	834
T7L*	6	50	17	162	28	338	43	578
T6-3	8	59	23	187	37	387	51	659

B : Average band height for sky line storage final

N : Number of unknowns

Figure 8. Colliding flow mesh

where u_1, u_2 are calculated values and u_{e1}, u_{e2} are exact values obtained from equation (23) and n is the total number of velocity unknowns.

In a similar manner, the pressure error norm is

$$E_p = \frac{\sum_{i=1}^{n_p} |p - p_e|}{n_p}, \quad n_p = \text{number of pressure components.}$$

Various mesh configurations and problem characteristics are given in Figure 8. The error norms E_u, E_p are given in Figures 9 and 10, respectively. The pressure and velocity accuracy of T7L is quite evident.

Cavity flow. To test the relative accuracy of these elements for non-linear flows, we chose the classical square cavity with a recirculating flow. The velocity components are zero on all sides,

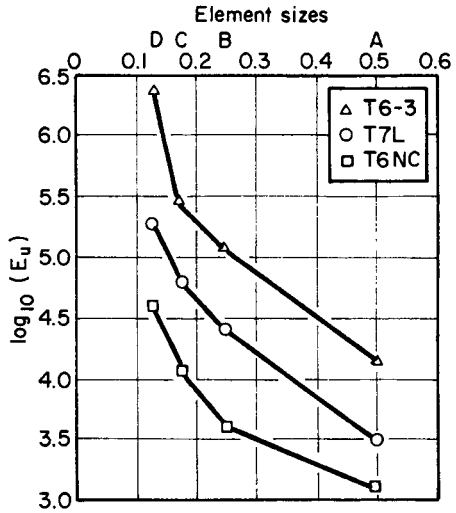

Figure 9. Velocity error

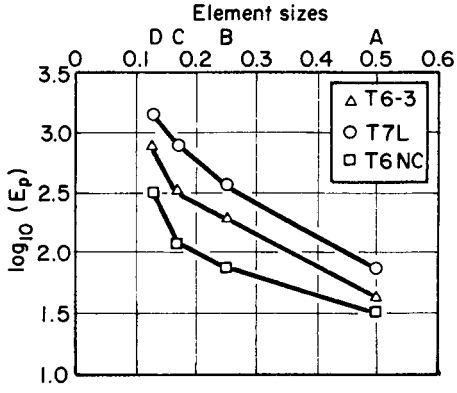

Figure 10. Pressure error

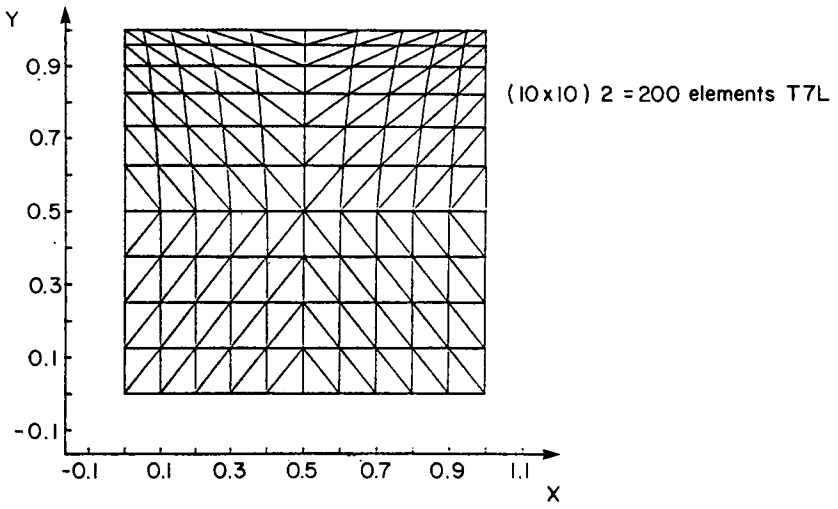

Figure 11. Cavity flow: Mesh configurations

except at the upper lid where horizontal velocity is imposed to be unity and normal velocity is zero.

We observed that the T7L element leads to superior velocity and pressure estimates as compared with other triangular elements. In Figures 11 and 12, we present only the results obtained with T7L for Reynolds numbers 100 and 400. The pressure values are normalized by $\bar{p} = (p - p(0{\cdot}5,0))Re/u_{\max}^2$ and the stream function is normalized by $\bar{\psi} = \psi/Re$.

Three-dimensional flow

Poiseuille flow for $Re = 0$. We employ H8N and H8 elements for studying a simple Poiseuille flow between two parallel plates. The purpose of this test is to observe the influence of distortion of element shapes on the velocity and pressure values. One should notice that the element H8 does not respect the LBB stability condition! The boundary conditions and the results for two mesh configurations are given in Figure 13. M1 is a rectangular $3 \times 3 \times 3$ mesh and M2 is like M1 but with a distortion of elements shapes produced by a 5 per cent displacement of the co-ordinates of the central node. One may observe from Figure 13 that there is a significant influence of distortion on the results of the H8 element, especially for pressure values as compared with the element H8N. If one employs the H8 element for 3-D studies, it is necessary to employ certain pressure filtering techniques.[23]

Three-dimensional recirculating cavity flow. A unit cavity with a sliding upper plate is studied, employing H8 and H8N elements. We use 224 elements with a mesh size of $8 \times 7 \times 4$ over a half cavity. The boundary conditions are shown in Figure 14 and various pressure and velocity profiles are shown in Figure 15. The pressure is normalized as $\bar{p} = (p - p(0,0,0))Re/u_{\max}^2$. The element employed by Reddy[24] and H8 are identical. It seems that discrepancy of results for u_2 in Figure 15 between Reddy and ourselves is primarily due to the presentation error in Reference 24. Since the element shape is rectangular, the velocity and pressure profiles for H8 show no oscillations or major errors as compared with H8N.

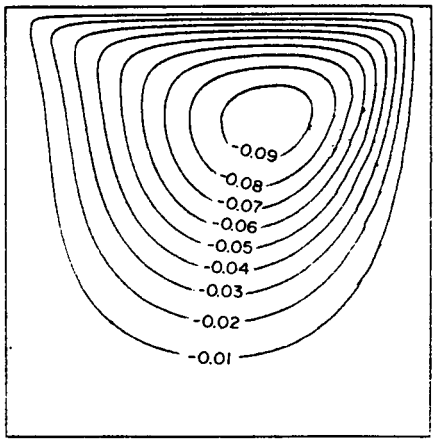

Streamlines at Re = 100

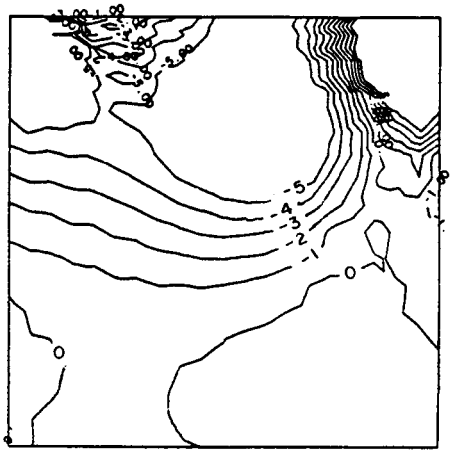

Pressure level plots at Re = 100

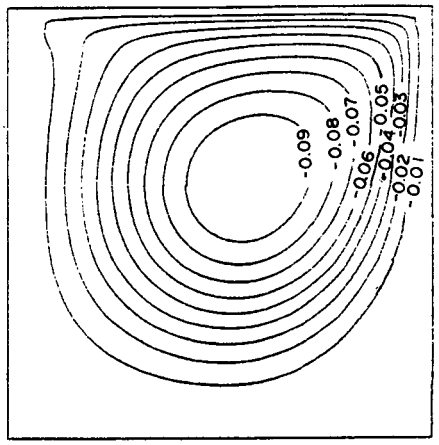

Streamlines at Re = 400

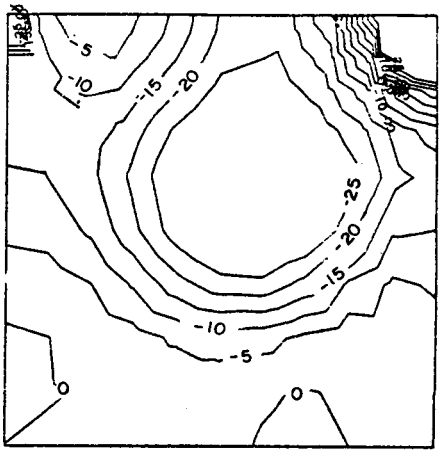

Pressure level plots at Re = 400

Figure 12. Pressure and stream function values for cavity flow

	H8	H8N
M_1	u : $O(10^{-6})$ p : $O(10^{-4})$	u : $O(10^{-3})$ p : $O(10^{-2})$
M_2	u : $O(10^{-3})$ p : $O(10^{1})$	u : $O(10^{-3})$ p : $O(10^{-2})$

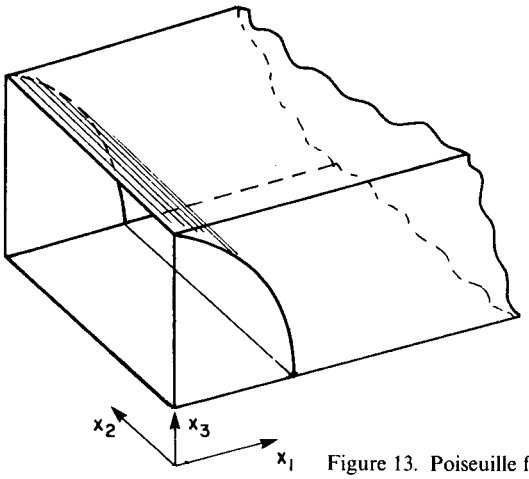

Dimensions $0 \le x_1 \le 1$
$0 \le x_2 \le 1$
$0 \le x_3 \le 0.5$

Boundary conditions

$x_1 = 0$ u_1 = profile parabolic
$u_2 = u_3 = 0$

$x_1 = 1$ u_1, u_2, u_3 free

$x_3 = 0.5$ $u_1 = u_2 = u_3 = 0$

$x_3 = 0$ $u_3 = 0$

Figure 13. Poiseuille flow

CONCLUDING REMARKS

We have presented a list of various penalty elements for two- and three-dimensional flows. Numerical results have been presented to test two triangular elements and two hexahedral elements.

Our experience with various triangular elements proposed in this study suggests that the element T7L gives probably the best results, both for velocity and pressure fields. This element becomes very efficient if the internal velocity components are condensed at the element level.

For three-dimensional elements, we have so far a limited experience, using only H8 and H8N elements for cavity flows and flows around a sphere. Our studies have shown that though H8N is oscillation-free, one can obtain acceptable results with the H8 element if certain pressure filtering is employed. Certainly, the element H8 is far simpler and more efficient numerically as compared with H8N.

A major problem for three-dimensional flow studies is the choice of an efficient solution strategy. We have so far employed variants of the Newton method, the industrial application of which is not efficient, owing to large matrix sizes and the computational effort involved in the construction and triangularization of matrices. It seems that any practical non-linear solvers will eventually employ the technique of conjugate gradients, least-square conditioning and, necessarily, a decomposition over space and velocity components.

At present, we are trying to develop efficient hexahedral and tetrahedral elements respecting the stability conditions. The basic idea seems to be the introduction of an internal node for velocity components, employing a C^0 field for pressure.

APPENDIX: VERIFICATION OF THE LBB CONDITION

We shall present a simple method of verification of the LBB condition adapted to discontinuous pressure approximation. It is assumed that the variational model satisfies the LBB condition in continuous form:

$$\sup_{u\in H_0^1} \frac{\int_V q \operatorname{div} \mathbf{u}\, dV}{\|u\|_{H_0^1}} > a\|q\|_{L^2}, \quad \forall q \in L^2, \quad a>0. \tag{24}$$

If the finite element approximation u_h defines 'continuously' the field u, (this is true for the type of finite element approximation employed normally), then an equivalent version of the discrete LBB condition is to verify the following relation:

$$\int_V q_h \operatorname{div} \mathbf{u}_h dV = \int_V q_h \operatorname{div} \mathbf{u} dV, \quad \text{for all} \quad q_h, \mathbf{u}_h, \mathbf{u} \tag{25}$$

where $q_h, \mathbf{u}_h$ are finite element approximations of q and $\mathbf{u}$, respectively.

For a discontinuous q_h field, equation (25) becomes

$$\int_E q_h \operatorname{div} \mathbf{u}_h dV = \int_E q_h \operatorname{div} \mathbf{u} dV \tag{26}$$

where E is the element volume.

We shall show how, for various types of elements presented in this study, equation (26) is verified.

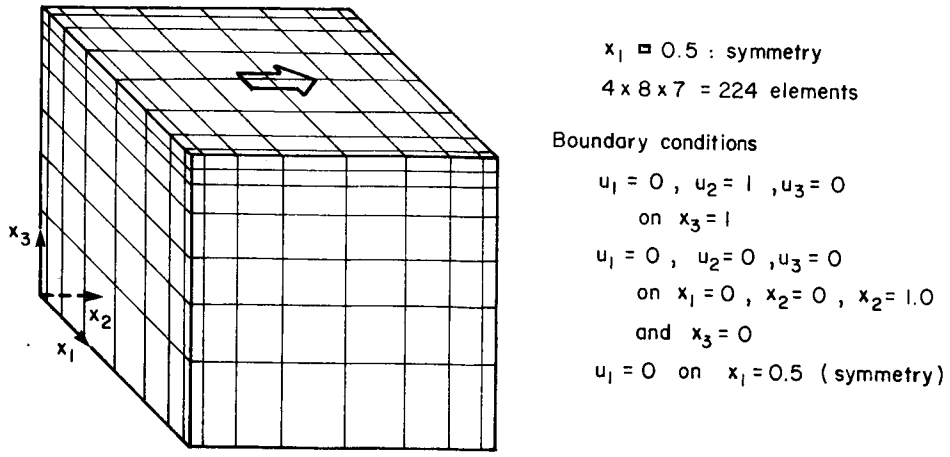

Figure 14. Mesh configuration and boundary conditions for cubic cavity flow

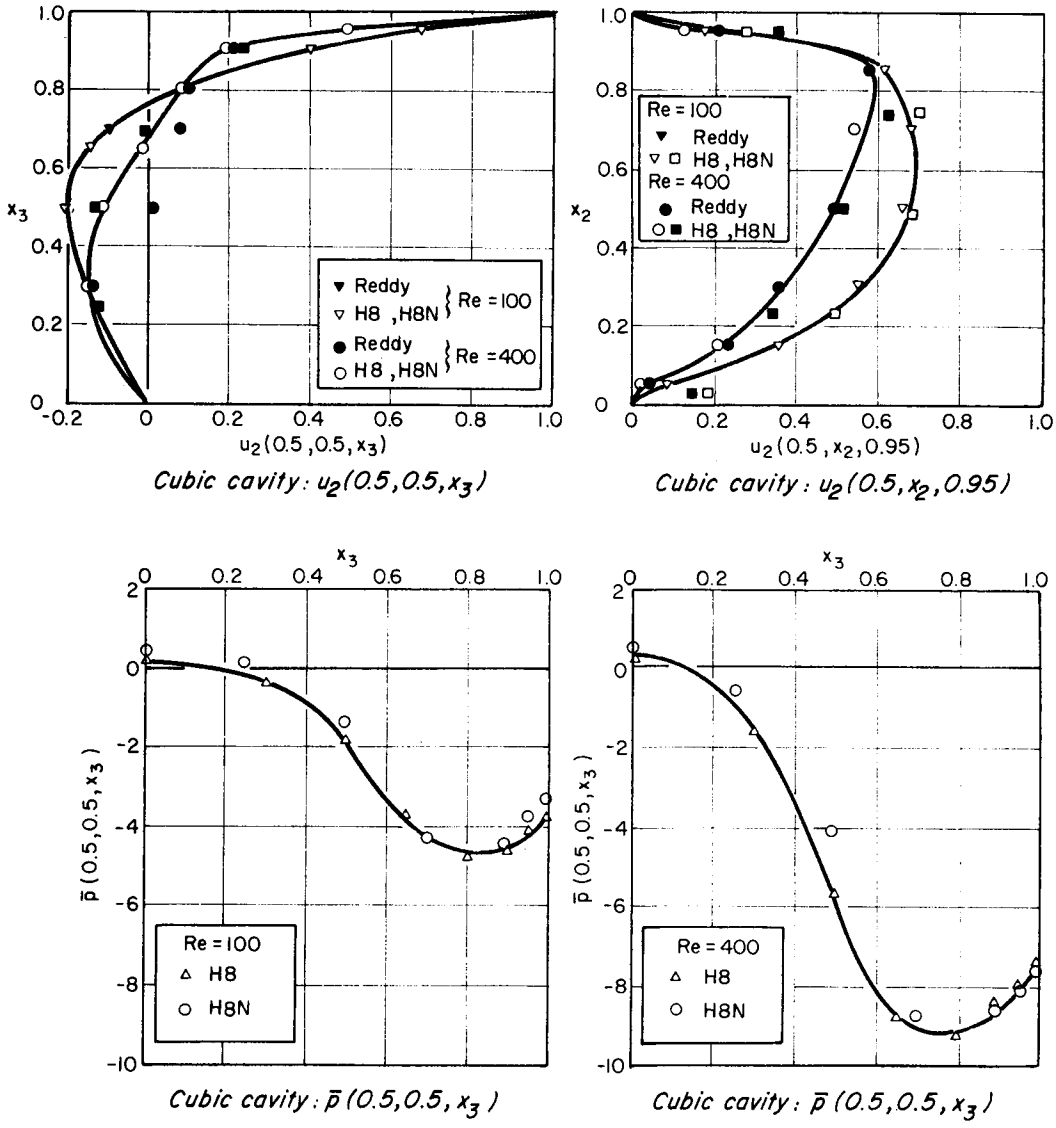

Figure 15. Pressure and velocity profiles for a cubic cavity

Elements with constant pressure

For constant pressure elements (2-D and 3-D), equation (26) becomes, after integration by parts (q_h constant)

$$\int_{\partial E} u_{nh} \mathrm{d}s = \int_{\partial E} u_n \mathrm{d}s \tag{27}$$

where ∂E is the boundary of an element E and u_n is the normal component of velocity.

In a more restricted sense,

$$\int_{\text{A-B}} u_{nh} \mathrm{d}s = \int_{\text{A-B}} u_n \mathrm{d}s, \tag{28}$$

where A-B represent any side or face of an element.

One may conclude that if an element has a normal velocity component associated with each face (3-D) or with each side (2-D), then equation (28) is always satisfied. For example, along a side of the element T6NC:

$$u_{nh} = N_{\text{A}} u_{\text{A}} + N_{\text{B}} u_{\text{B}} + N_{\text{m}} u_{\text{m}}$$

Equation (28) becomes

$$\int_{\text{A-B}} (N_{\text{A}} u_{\text{A}} + N_{\text{B}} u_{\text{B}}) \mathrm{d}s + \int_{\text{A-B}} N_{\text{m}} u_{\text{m}} \mathrm{d}s = \int_{\text{A-B}} u_n \mathrm{d}s$$

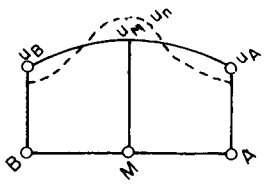

One can locally adjust u_{m} for any values of $u_{\text{A}}, u_{\text{B}}, u_{\text{n}}$ since the mid-side node is shared only by the side A-B, thus satisfying (28). A similar reasoning is applied to 3-D elements.

Elements with linear pressure

For 2-D elements, the linear pressure may be written as

$$p = a + b\xi + c\eta \tag{29}$$

Equation (26) should be satisfied for the terms in ξ and η and (28) for the constant term. This is possible if

(a) a normal velocity component is associated with each side (2-D) or each face (3-D)
(b) a node containing all velocity components is associated with the interior of an element (a bubble function).

The proof follows similar lines as for constant pressure, except that equation (26) is employed to verify for terms ξ, η, i.e.

$$\int_E \xi A \mathrm{d}V = \int_E \xi \,\mathrm{div}\,\mathbf{u}\, \mathrm{d}V$$

$$\int_E \eta A \mathrm{d}V = \int_E \eta \,\mathrm{div}\,\mathbf{u}\, \mathrm{d}V, \tag{30}$$

where

$$A = \frac{\partial}{\partial x}\langle \mathbf{N} \rangle \{\mathbf{u}\} + \frac{\partial N_{\text{l}}}{\partial x} u_{\text{l}} + \frac{\partial}{\partial y}\langle \mathbf{N} \rangle \{\mathbf{v}\} + \frac{\partial N_{\text{l}}}{\partial y} v_{\text{l}}.$$

$\{\mathbf{u}\}$; $\{\mathbf{v}\}$ contains the nodal velocity components shared by neighbouring elements, $\langle \mathbf{N} \rangle$ is the

corresponding approximating function, N_I is the internal bubble function associated with internal components u_I, v_I. In such a case it is always possible to choose u_I, v_I to satisfy these two relations.

BIBLIOGRAPHY

1. G. Dhatt and G. Touzot, *Une Présentation de la méthode des Éléments Finis*, Maloine, Paris, 1981; English translation: *Finite Element Method Displayed*, Wiley, 1984.
2. J. F. Cochet, 'Modélisation d'écoulements stationnaires et non stationnaires par éléments finis', *Thèse de Docteur-ingénieur*, Université de Compiègne, France, 1979.
3. D. S. Malkus and T. J. R. Hughes, 'Mixed finite elements methods, reduced and selective integration: a unification of concepts', *Comp. Meth. in Applied Mechanics and Engineering*, **15**, 63–81 (1978).
4. A. Soulaimani, 'Nouveaux aspects de l'application de la méthode des éléments finis en hydrodynamique', *M.Sc. Thesis*, Civil Engineering, Laval University, 1984.
5. C. Taylor and P. Hood, 'Numerical solution of the Navier–Stokes equations using the finite element technique', *Comp. and Fluids*, **1**, 1–28 (1973).
6. G. Dhatt and G. Hubert, 'Some new penalty elements for incompressible flows', *3rd International Conference on Numerical Methods in Laminar and Turbulent Flow*, Seattle, U.S.A., 8–11, August 1983.
7. R. L. Sani, M. S. Engelman, P. M. Gresho and M. Bercovier, 'Consistent vs reduced integration penalty methods for incompressible media using several old and new elements', *Int. j. numer. methods fluids*, **2**, 25–42 (1982).
8. J. T. Oden, 'Penalty methods and selective reduced integration for stokesian flows', *3rd International Conference on Finite Elements in Flow Problems*, Banff, Alberta, Canada, 1980.
9. O. C. Zienkiewicz and J. C. Heinrich, 'A unified treatment of steady-state shallow-water and two-dimensional Navier-Stokes equations finite element penalty function approach', *Comp. Methods in Applied Engineering*, 673–698 (1979).
10. O. A. Ladyszhenskaya, *The Mathematical Theory of Viscous Incompressible Flows*, Gordon and Breach, New York, 1969.
11. F. Brezzi, 'On the existence, uniqueness and approximation of saddle point problems arising from Lagrange multipliers', *R.A.I.R.O.*, série rouge, **R2**, 129–151 (1974).
12. I. Babuska, 'Error bounds for finite elements method', *Num. Math.*, **16**, 322–333 (1971).
13. O. C. Zienkiewicz, 'Constrained variational principles and penalty function methods in finite element analysis', *Lecture notes in Mathematics*, Springer, 1974, p. 363.
14. J. F. Cochet, G. Dhatt, G. Hubert and G. Touzot, 'River and estuary flows by a new penalty element', *4th International Symposium on Finite Elements in Flow Problems*, Tokyo, Japan, 26–29 July 1982.
15. J. T. Oden, N. Kikuchi and Y. J. Song, 'Penalty finite element methods for the analysis of stokesian flows', *Comp. Meth. Appl. Mech. Eng.*, **31**, 297–329 (1982).
16. J. N. Reddy, 'On penalty function methods in the finite elements analysis of flow problems', *Int. j. numer. methods fluids*, **2**, 151–171 (1978).
17. M. Fortin, 'Old and new finite elements for incompressible flows'. *Int. j. numer. methods fluids*, **1**, 347–364 (1981).
18. M. Geradin, S. Idelsohn and M. Hogge, 'Computational strategies for the solution of large nonlinear problems via quasi-Newton methods', *Comp. & Structures*, **13**, 73–81 (1983).
19. G. Hubert, 'Modélisation d'écoulements de fluides incompressibles par la méthode des éléments finis', *Thèse de Docteur-ingénieur*, Division MNM, Université de Compiègne, France, 1984.
20. M. Jaeger, 'Méthode quasi-Newton pour la résolution de problèmes non-linéaires par éléments finis', *Rapport de DEA de Mécanique et calcul des structures*, 1983, Université de Compiègne, Div. MNM, France.
21. R. Glowinski and J. Periaux, 'Finite elements, least squares and domains decomposition methods for the numerical solution of non-linear problems in fluid dynamics', *C.I.M.E., Numerical Methods in Fluids Dynamics*, Cone, Italy, 1983.
22. J. Periaux, 'Résolution de quelques problèmes non-linéaires en aérodynamique par des méthodes d'éléments finis et de moindres carrés fonctionnels', *Thèse de 3e cycle*, Université de Paris VI, 1979.
23. R. L. Sani, P. M. Gresho, R. L. Lee and D. F. Griffiths, 'The cause and cure (?) of the spurious pressures generated by certain FEM solutions of the incompressible Navier–Stokes equations', *Int. j. numer. methods fluids*, Part 1, **1**, 17–43 (1981); Part II, **2**, 171–204 (1981).
24. J. N. Reddy, 'Penalty finite element analysis of 3D Navier–Stokes equations', *Comp. Meth. Appl. Mech. Eng.*, **35**, 87–106 (1982).
25. M. Bercovier, 'Perturbation of mixed variational problems, applications to mixed finite element methods', *R.A.I.R.O.*, **12**, 211–236 (1978).
26. O. R. Burgraff, 'Analytical and numerical studies of the structure of steady separated flows', *J. Fluid Mech.*, **24**, 113–151 (1966).
27. J. C. Heinrich and R. S. Marshall, 'Viscous incompressible flow by a penalty function finite element method', *Comp. and Fluids*, **9**, 73–83 (1981).
28. T. J. R. Hughes, 'A simple scheme for developing upwind finite elements', *Int. j. numer. methods fluids*, **12**, 1359–1365 (1978).